

# Eclipse Timings of the LMXB XTE J1710-281: Orbital Period Glitches

Chetana Jain<sup>1\*</sup> and Biswajit Paul<sup>2</sup>

<sup>1</sup>*Hans Raj College, University of Delhi, Delhi 110007, India*

<sup>2</sup>*Raman Research Institute, Sadashivnagar, C. V. Raman Avenue, Bangalore 560080, India*

## ABSTRACT

We present an X-ray eclipse timing analysis of the transient low mass X-ray binary XTE J1710-281. We report observations of 57 complete X-ray eclipses, spread over more than a decade of observations, made with the proportional counter array detectors aboard the *RXTE* satellite. Using the eclipse timing technique, we have derived a constant orbital period of 0.1367109674 (3) d, during the period from MJD 52132 upto MJD 54410; and  $1\sigma$  limits of  $-1.6 \times 10^{-12} \text{ d d}^{-1}$  and  $0.2 \times 10^{-12} \text{ d d}^{-1}$ , on the period derivative,  $\dot{P}_{orb}$ . This puts constraints on the minimum timescale of secular orbital period evolution ( $P_{orb}/\dot{P}_{orb}$ ) of  $2.34 \times 10^8 \text{ yr}$  for a period decay and  $18.7 \times 10^8 \text{ yr}$  for a period increase. We also report detection of two instances of discontinuity in the mid-eclipse time, one before and one after the above MJD range. These results are interpreted as three distinct epochs of orbital period in XTE J1710-281. We have put lower limits of 1.4 ms and 0.9 ms on orbital period change ( $\Delta P_{orb}$ ) at successive epochs. The detection significance of the two orbital period glitches are  $11\sigma$  and  $4\sigma$  respectively. The sudden changes in orbital period is very similar in nature to that observed in EXO 0748-676, though their magnitude is much smaller in XTE J1710-281.

**Key words:** accretion, accretion discs, binaries: eclipsing, binaries: general, stars: individual: XTE J1710-281, stars: neutron, X-rays: stars

## 1 INTRODUCTION

XTE J1710-281 is a transient Low Mass X-ray Binary (LMXB) which was discovered in 1998 by the Rossi X-ray Timing Explorer (*RXTE*), and is likely to be associated with the ROSAT source 1RXS J171012.3-280754 (Markwardt et al. 1998). It is a highly variable source and several bursts have been reported to occur (Markwardt et al. 2001; Galloway et al. 2008). The system has an orbital period of 3.28 hr (Markwardt et al. 2001) and the light curve shows dipping phenomena which could be due to occultations in the outer regions of the accretion disk as seen in many other high inclination LMXBs (White & Swank 1982).

XTE J1710-281 is a poorly studied LMXB. Being in a binary system, the orbital period of XTE J1710-281 is expected to change, due to redistribution of the angular momentum arising from interaction between the components of the binary system. The orbit can evolve due to various mechanisms, such as, mass transfer within

the system due to Roche lobe overflow, tidal interaction between the components of the binary system, gravitational wave radiation, magnetic braking, (Rappaport et al. 1983; Hurley et al. 2002) and X-ray irradiated wind outflow (Ruderman et al. 1989). The measurement of orbital period derivative and hence the orbital evolution is therefore, important to understand the physical processes occurring in the system.

Orbital evolution can be determined by several techniques. Measurement of pulse arrival time delay, is one of the methods used to determine the evolution of the binary orbits (Deeter et al. 1991; Paul et al. 2004, 2007). The method of pulse folding and  $\chi^2$  maximization with a varying orbital ephemeris, has also been used to determine the orbital evolution (Paul et al. 2002; Jain et al. 2007). Both these methods are well established and statistically at par. However, to determine the pulse arrival times, the data-length for each sample should be kept small so as to avoid significant smearing of pulse phase due to orbital motion. In the case of faint sources, or in the case of observation made with a small photon collection area (e.g. with focussing optics), a small integration time may be insufficient for measurement of pulse arrival time. In such a case, maximisation of pulse

\* E-mail: chetana.jain11@gmail.com (CJ); bpaul@rri.res.in (BP)

detection by varying the orbital ephemeris is an effective technique as the entire data set is used together (Paul et al. 2002). Eclipse timing is another technique, used to determine the orbital evolution of LMXBs (Wolff et al. 2009; Jain et al. 2010). In some sources, in the absence of pulsations or eclipses, orbital period derivative has been measured with some stable orbital intensity modulation features (4U 1820-30: Chou & Grindlay (2001); Cyg X-3: Singh et al. (2002)).

XTE J1710-281 is one of the very few LMXBs, where full, sharp X-ray eclipses have been observed. The other systems being, EXO 0748-676 (Wolff et al. 2002), GRS J1747-312 (in't Zand et al. 2003), MXB 1658-298 (Cominsky & Wood 1989) and AX J1745.6-2901 (Maeda et al. 1996). Among these sources, EXO 0748-676 (Parmar et al. 1986; Wolff et al. 2002) is the only system in which a large number of eclipses have been timed with high accuracy (Wolff et al. 2009). In case of GRS J1747-312 and AX J1745.6-2901, the eclipse duration is too long ( $\sim 43$  minutes and  $\sim 23$  minutes, respectively, in't Zand et al. (2003); Porquet et al. (2007)) to carry out monitoring measurements. AX J1745.6-2901 is located near a bright source, which puts strong constraints on the timing analysis. The fifth source, MXB 1658-298 has been mostly in inactive state, since its discovery (Wachter et al. 2000; Oosterbroek et al. 2001). The LMXB XTE J1710-281 has a fairly small eclipse duration and has been persistently active since its discovery. This makes it an ideal source to investigate the orbital evolution.

In this work, we have used the sharp eclipses of XTE J1710-281 as timing markers to determine the orbital period of the system. By measuring the mid-eclipse times, over a long time baseline of  $\sim 11$  years, we can determine the change in the orbital period and hence estimate the orbital evolution of the system.

## 2 OBSERVATIONS AND ANALYSIS

Data for the present analysis were obtained from observations made with the Proportional Counter Array (PCA) on board the Rossi X-ray Timing Explorer (*RXTE*) satellite (Bradt et al. 1993). The *RXTE*-PCA consists of an array of five collimated xenon/methane multianode proportional counter units (PCU) with a total photon collection area of  $6500 \text{ cm}^2$  (Jahoda et al. 1996, 2006), depending on the number of PCUs ON. The entire analysis was done using FTOOLS from the astronomy software package HEASOFT-ver 6.10. The PCA data collected in the event mode and the Good Xenon mode, were used to generate the light curves, using the FTOOL-SEEXTRACT. The analysis was done in the energy band 2–20 keV. The background was estimated using the FTOOL-PCABACKEST. Faint source model was taken from the *RXTE* website ([http://heasarc.gsfc.nasa.gov/docs/xte/pca\\_news.html](http://heasarc.gsfc.nasa.gov/docs/xte/pca_news.html)). Thereafter, the background subtracted light curves were barycenter corrected using the FTOOL-FAXBARY.

We have analyzed all the *RXTE*-PCA archival data, which covered a full X-ray eclipse. However, since this is a bursting source, we ignored few eclipses, where bursts occurred close to the ingress and egress phase of the eclipse. From data spread over  $\sim 11$  years (1999-2010), we have found

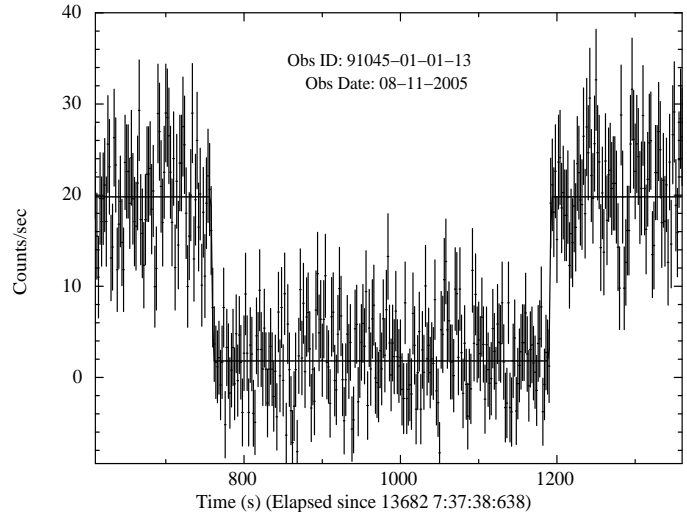


**Figure 1.** A sample of 2–20 keV, background subtracted light curve of XTE J1710-281, binned with 2 s and including an eclipse lasting for about 428 s. The line represents the best fit five-parameter model for the light curve. The best fit had a  $\chi^2$  of 381 for 375 d.o.f.

57 complete eclipses. Table 1 gives the observation IDs of all the 57 eclipses, observed with *RXTE*-PCA. In Figure 1, we have shown a sample background subtracted light curve of XTE J1710-281 (Obs ID: 91045-01-01-13), binned with 2 seconds and including an eclipse lasting for  $\sim 420$  s, excluding the ingress and egress phase.

For most of the observations, apart from a few type-I X-ray bursts, the out-of-eclipse count rate did not seem to have any significant variability. Therefore, the variable components of the light curve around the eclipse phase are, the pre-ingress ( $C_{pre-ingress}$ ), eclipse ( $C_{eclipse}$ ), and post-egress ( $C_{post-egress}$ ) count rates; the ingress ( $\Delta t_{in}$ ) and egress ( $\Delta t_{eg}$ ) duration, the eclipse duration ( $\Delta t_{ecl}$ ) and the mid-eclipse time. Considering all the components to be freely variable, we first fitted a seven-parameter ramp and step model to the eclipse phase (similar to Wolff et al. (2009)). It was found that the value of  $C_{pre-ingress}$  and  $C_{post-egress}$  were similar and the eclipse ingress and egress duration were also similar withing errors. The parameter space, thus got reduced to five: the pre-ingress and the post-egress count rate ( $C_{pre-in-post-eg}$ ), the eclipse count rate, the ingress and egress duration ( $\Delta t_{in,eg}$ ), the eclipse duration ( $\Delta t_{ecl}$ ), and the mid-eclipse time. The average eclipse duration in XTE J1710-281 is  $\sim 420$  s; and for the model fitting,  $\sim 150$  seconds of data was taken before and after the eclipse phase. It was also seen that the error in the mid eclipse time measurement was smaller when the five-parameter model was used. The best fit model for the eclipse profile in Figure 1, is shown with a solid line. The best fit had a  $\chi^2$  of 381 for 375 degrees of freedom.

All the 57 X-ray eclipse light curves were fitted with a five-parameter ramp function, as described above. The mid-eclipse times and the corresponding  $1\sigma$  errors were determined. The results are given in Table 1. The errors in the mid-eclipse times vary between 0.000006 d to 0.000064 d, i.e. 0.5 s to 5.5 s. This is mainly due to difference in the relative count rates of the source and the background, and partly due to the number of detectors ON. The orbit numbers are

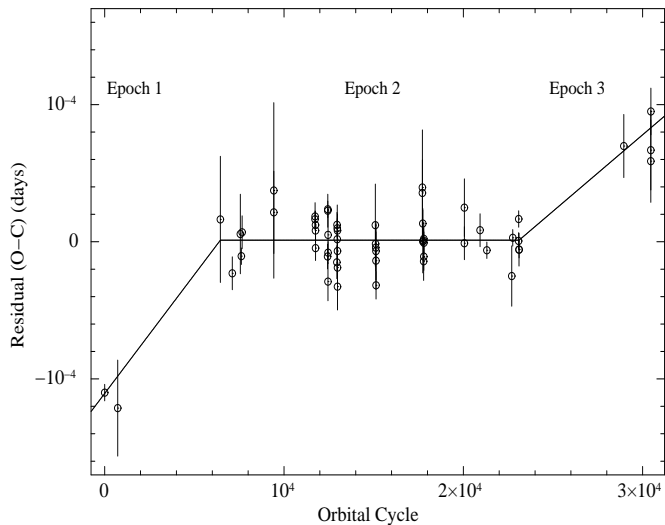


**Figure 2.** The observed minus calculated times (residuals, O-C) for eclipses observed in XTE J1710-281 during 1999-2010, obtained from *RXTE*-PCA observations. The O-C variation is plotted as a function of orbital cycle. The three distinct orbital period epochs are mentioned.

with respect to the first eclipse detected in the *RXTE*-PCA data. We fitted a constant and a linear model to the eclipse measurements between MJD 52132 - 54410. The results of the fit are given in Table 2. We obtained an orbital period of 0.1367109674 (3) d (epoch MJD 51250.924540 (4)) and have derived  $1\sigma$  limits of  $0.2 \times 10^{-12} \text{ d d}^{-1}$  and  $-1.6 \times 10^{-12} \text{ d d}^{-1}$ , on the orbital period derivative ( $\dot{P}_{orb}$ ). The  $\chi^2$  of the fit was 74 for 51 d.o.f. Before and after the above mentioned MJD range, we found shifts in the mid-eclipse times. We refer to these shifts as three epochs in the orbital period.

Figure 2 shows the “observed minus calculated” (O - C) diagram for all the eclipse measurements of XTE J1710-281, obtained after subtracting the linear component obtained from epoch 2. The three different epochs of orbital period is evident. It is obvious from the figure that a polynomial function consisting of linear ( $P_{orb}$ ), quadratic ( $P_{orb}^2$ ), cubic ( $P_{orb}^3$ ) etc terms cannot be fitted to the observed dataset. A piecewise linear function could be more appropriate. But, there are few observations in epoch 1 and epoch 3, hence one cannot determine the orbital period during epoch-1 and epoch-3 with very high accuracy. However, from our observations, we have put lower limits on orbital period changes of  $\Delta P = 1.4 \text{ ms}$  ( $1.7 \times 10^{-8} \text{ d}$ ) between epoch-1 and epoch-2; and a  $\Delta P = 0.9 \text{ ms}$  ( $1.1 \times 10^{-8} \text{ d}$ ) between epoch-2 and epoch-3. The detection significance of the two orbital period glitches are  $11\sigma$  and  $4\sigma$  respectively.

We have also created average eclipse profiles for the three epochs by combining all the corresponding eclipse light curves. The eclipse light curves were co-added using the orbital period and epoch given in Table 2. The folded profiles are shown in the top panel of Figure 3. The best fit ramp function is also shown for the eclipse profile of epoch 2. The best fit had a  $\chi^2$  of 689 for 650 degrees of freedom (d.o.f). The bottom panels of the same figure shows the eclipse ingress and egress profiles. It is clear from Figure 3 that the time of ingress and egress of eclipse, during the

three epochs is shifted in phase while the eclipse duration has remained nearly same.

### 3 DISCUSSION

Measurements of change in orbital period of an LMXB, is a crucial diagnostic to understand the accretion processes occurring in a binary system; and their effect on the system parameters. And the orbital period can be very well determined by time connecting a stable fiducial marker in the light curve of the binary system. We have analyzed 57 full X-ray eclipses of XTE J1710-281, observed by the *RXTE* satellite. The observations cover more than 30000 binary orbits spread over  $\sim 11$  years. A five-component model was fit to each eclipse profile and the mid-eclipse times and the corresponding errors determined. We have determined an orbital period of 0.1367109674 (3) d and limits on the period derivative of  $-1.6 \times 10^{-12} \text{ d d}^{-1}$  and  $0.2 \times 10^{-12} \text{ d d}^{-1}$ , i.e., limits on the timescale of secular orbital period evolution,  $P_{orb}/\dot{P}_{orb}$ , of  $2.34 \times 10^8 \text{ yr}$  for a period decay and  $18.7 \times 10^8 \text{ yr}$  for a period increase, respectively, during the period from MJD 52132 to MJD 54410.

The variation in the orbital ephemerides of XTE J1710-281, is significantly different from that seen in most of the other LMXB systems, such as, 4U 1820-303 (Chou & Grindlay 2001), SAX J1808.4-3658 (Jain et al. 2007), Her X-1 (Paul et al. 2007), X 2127+119 (Homer & Charles 1998) and 4U 1822-37 (Jain et al. 2010). During the period from MJD 52132 to MJD 54410, the limits on the orbital period derivative of XTE J1710-281, is more than an order of magnitude smaller than those measured in the other LMXBs (4U 1820-303 ( $3.5 \times 10^{-8} \text{ yr}^{-1}$ ), SAX J1808.4-3658 ( $1.3 \times 10^{-8} \text{ yr}^{-1}$ ), Her X-1 ( $-2 \times 10^{-7} \text{ yr}^{-1}$ ), X 2127+119 ( $9 \times 10^{-7} \text{ yr}^{-1}$ ) and 4U 1822-37 ( $2.0 \times 10^{-7} \text{ yr}^{-1}$ )). Outside the above MJD range, the observed trend in the residual (O - C) behaviour of XTE J1710-281, is also different from that seen in the aforementioned LMXBs.

The observed O - C variation strongly resemble the one seen in EXO 0748-676 (Wolff et al. 2009). Interestingly, of the known LMXBs with well determined eclipse times, EXO 0748-676 and XTE J1710-281 have shortest duration of the eclipse, making it easier to monitor with X-ray observatories. Though fewer eclipses have been observed in XTE J1710-281, as opposed to more than 400 complete eclipses seen from EXO 0748-676 (Wolff et al. 2009), the mid-eclipse times measured with *RXTE*-PCA are accurate enough to enable detection of very small orbital period glitches.

Magnetic field cycling of the secondary star is assumed to be the likely cause for the observed orbital period glitches in EXO 0748-676 (Wolff et al. 2009). It is proposed that magnetic activity associated with the secondary star could be responsible for sudden changes in the orbital period. If the secondary star associated with XTE J1710-281 has strong, changing, magnetic activity, it can lead to changes in the structure of secondary star. A changing gravitational quadrupole moment can result into changes in the orbital period of the binary system (Lanza & Rodono 1999; Tauris & van den Heuvel 2006). However, in case of XTE J1710-281, the optical counterpart has been discovered (Ratti et al. 2010) but the type of the companion star

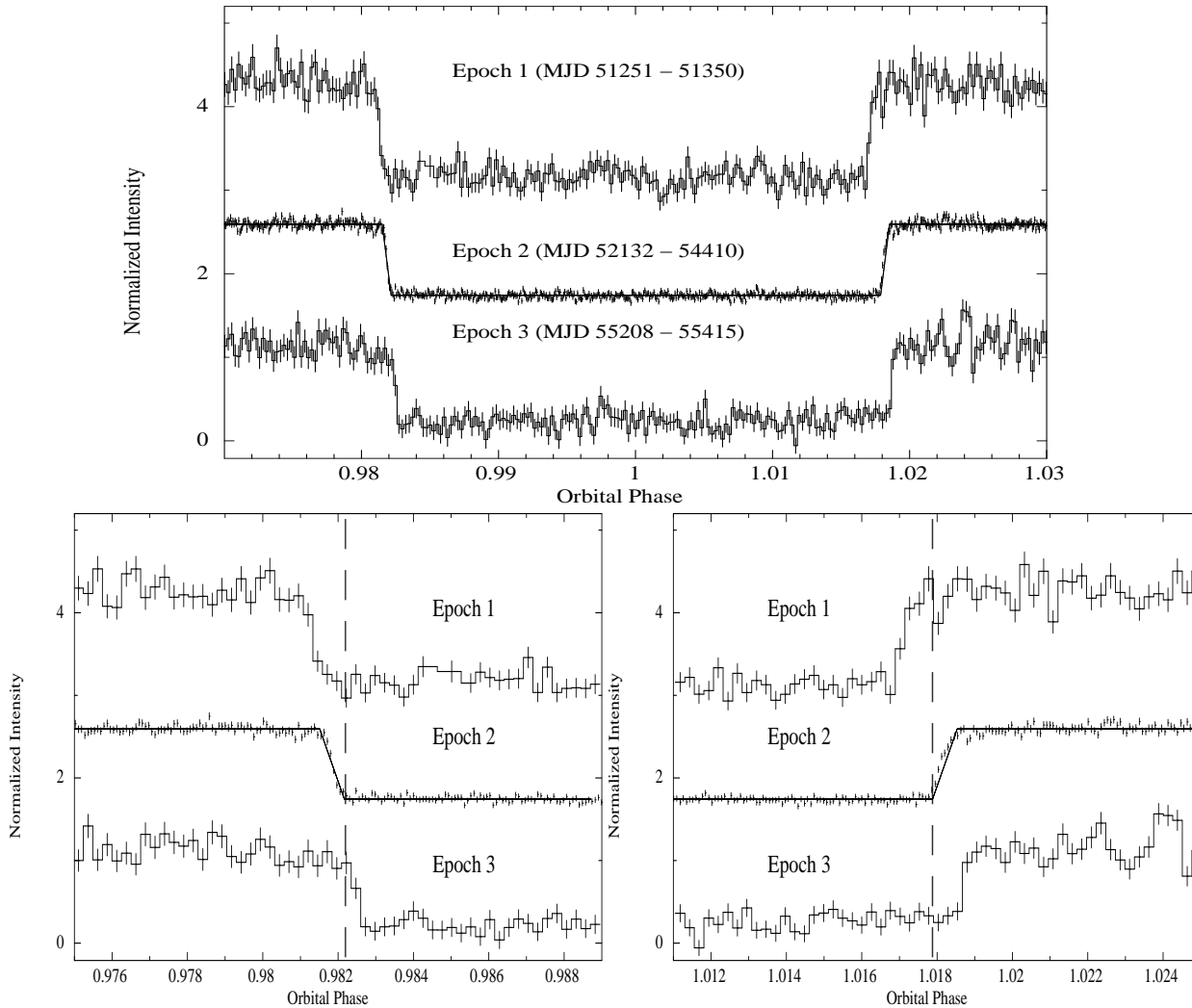


**Figure 3.** A sample of 2–20 keV folded light curves of XTE J1710-281. The light curves were folded with a period of 0.1367109674 d at an epoch of MJD 51250.924540. The normalised intensities during epoch-1 and epoch-2 have been rescaled, by adding constant numbers to the curves. The solid line in the middle light curve (epoch 2) shows the best fit five-parameter model to the X-ray eclipse. The best fit had a reduced  $\chi^2$  of 689 for 650 d.o.f. The top panel shows the complete eclipse, whereas, the bottom panels show the ingress and egress of the eclipse phase.

is not yet known. Therefore, it is difficult to make a statement on the probable cause for the changing orbital period of XTE J1710-281.

We emphasise that if magnetic cycling of the binary components is indeed a reason behind the observed epochs of orbital period, then long term monitoring of XTE J1710-281, is required to determine the timescales of magnetic cycling of the secondary star. It may also be useful to foretell the distinct orbital period epochs of XTE J1710-281, if any. Lastly, the forthcoming Indian-satellite, *ASTROSAT* with a very large area X-ray proportional counter (Paul 2009) could be a boon in determining the orbital parameters of the system.

#### ACKNOWLEDGMENTS

This research has made use of data obtained from the High Energy Astrophysics Science Archive Research Center

(HEASARC), provided by NASA’s Goddard Space Flight Center.

#### REFERENCES

- Bradt H. V., Rothschild R. E., Swank, J. H., 1993, *A&AS*, 97, 1  
 Chou Y., Grindlay J. E., 2001, *ApJ*, 563, 934  
 Cominsky L. R., Wood K. S., 1989, *ApJ*, 337, 485  
 Deeter, J. E., Boynton, P. E., Miyamoto, S., Kitamoto, S., Nagase, F., Kawai, N., 1991, *ApJ*, 383, 324  
 Galloway D. K., Muno M. P., Hartman J. M., Psaltis D., Chakrabarty D., 2008, *ApJS*, 179, 360  
 Homer L., Charles P. A., 1998, *New Astron.*, 3, 435  
 Hurley J. R., Tout C. A., Pols O. R., 2002, *MNRAS*, 329, 897  
 in’t Zand J. J. M., Hulleman F., Markwardt C. B., Mendez M., Kuulkers E., Cornelisse R., Heise J., Strohmayer T. E., Verbun, F., 2003, *A & A*, 406, 233

**Table 1.** Mid Eclipse Time measurements of XTE J1710-281.

<i>RXTE</i> Observation ID	Orbital Cycle	Mid eclipse time MJD (d)	$1\sigma$ Uncertainty (d)
40407-01-03-00	1	51251.061141	0.000006
40135-01-40-00	728	51350.450003	0.000035
60049-01-01-03	6452	52132.983718	0.000046
60049-01-03-00	7118	52224.033183	0.000012
60049-01-04-00	7567	52285.416436	0.000029
60049-01-05-00	7623	52293.072234	0.000006
60049-01-06-00	7667	52299.087534	0.000012
60049-01-07-010	9431	52540.245711	0.000064
60049-01-07-01	9432	52540.382406	0.000030
80045-01-01-00	11732	52854.817626	0.000006
80045-01-01-01	11733	52854.954339	0.000010
80045-01-01-03	11756	52858.098681	0.000009
80045-01-01-04	11757	52858.235396	0.000010
80045-01-01-05	11760	52858.645512	0.000009
80045-01-02-00	12432	52950.515276	0.000009
80045-01-02-01	12444	52952.155841	0.000012
80045-01-02-03	12445	52952.292553	0.000006
80045-01-02-02	12454	52953.522899	0.000014
80045-01-02-04	12455	52953.659644	0.000019
80045-01-02-05	12456	52953.796342	0.000008
80045-01-03-00	12947	53020.921420	0.000012
80045-01-03-01	12957	53022.288557	0.000009
80045-01-03-02	12970	53024.065797	0.000017
80045-01-03-03	12971	53024.202500	0.000015
80045-01-03-04	12982	53025.706300	0.000012
80045-01-03-05	12983	53025.843038	0.000012
80045-01-03-06	12984	53025.979734	0.000008
80045-01-03-07	12985	53026.116419	0.000017
80045-01-04-00	15096	53314.713316	0.000030
80045-01-04-01	15107	53316.217123	0.000013
80045-01-04-02	15115	53317.310808	0.000017
80045-01-04-05	15129	53319.224759	0.000021
80045-01-04-06	15130	53319.361463	0.000021
80045-01-04-07	15131	53319.498156	0.000010
91045-01-01-00	17718	53673.169500	0.000042
91045-01-01-01	17719	53673.306207	0.000024
91045-01-01-02	17740	53676.177102	0.000023
91045-01-01-03	17741	53676.313826	0.000011
91045-01-01-13	17785	53682.329096	0.000009
91045-01-01-14	17786	53682.465792	0.000014
91045-01-01-15	17797	53683.969629	0.000012
91045-01-01-16	17798	53684.106327	0.000010
91045-01-01-17	17799	53684.243048	0.000008
91018-01-01-00	20059	53993.209860	0.000021
91018-01-01-00	20060	53993.346545	0.000012
91018-01-02-00	20934	54112.831940	0.000012
91018-01-03-01	21314	54164.782093	0.000006
93052-01-01-01	22700	54354.263475	0.000022
91018-01-07-04	22758	54362.192739	0.000006
91018-01-08-01	23086	54407.033934	0.000006
91018-01-08-01	23087	54407.170661	0.000006
91018-01-08-03	23107	54409.904858	0.000012
91018-01-08-03	23108	54410.041569	0.000006
94314-01-01-00	28952	55208.980538	0.000023
94314-01-06-00	30454	55414.320400	0.000030
94314-01-06-00	30455	55414.457119	0.000029
94314-01-06-01	30461	55415.277413	0.000017

**Table 2.** Orbital ephemerides of XTE J1710-281.

Parameter	Best fit value from present analysis
$T_0$ (MJD)	51250.924540 (4)
$P_{orb}$ (d)	0.1367109674 (3)
$\dot{P}_{orb}$ ( $10^{-12}$ d d $^{-1}$ )	$-1.6 \leq \dot{P}_{orb} \leq 0.2$
$P_{orb}/\dot{P}_{orb}$ ( $10^8$ yr)	$-2.34 \leq P_{orb}/\dot{P}_{orb} \leq 18.7$

- Jahoda K., Swank J. H., Giles A. B., Stark M. J., Strohmayer T., Zhang W., Morgan E. H., 1996, SPIE, 2808, 59
- Jahoda K., Markwardt C. B., Radeva Y., Rots A. H., Stark M. J., Swank J. H., Strohmayer T. E., Zhang W., 2006, ApJS, 163, 401
- Jain C., Dutta A., Paul B., 2007, J. Astrophys. Astron., 28, 197
- Jain C., Paul B., Dutta A., 2010, MNRAS, 409, 755
- Lanza, A. F., Rodono, M., 1999, A&A, 349, 887
- Maeda Y., Koyama K., Sakano M., Takeshima T., Yamauchi S., 1996, PASJ, 48, 417
- Markwardt C. B., Marshall F. E., Swank J., Takeshima T., 1998, IAUC, 6998, 2
- Markwardt C. B., Swank J. H., Strohmayer T. E., 2001, AAS, 199, 2704
- Oosterbroek T., Parmar A. N., Sidoli L., in't Zand J. J. M., Heise J., 2001, A & A, 376, 532O
- Parmar A. N., White N. E., Giommi P., Gottwald M., 1986, ApJ, 308, 199
- Paul B., Nagase F., Endo T., Dotani T., Yokogawa J., Nishiuchi M., 2002, ApJ, 579, 411
- Paul B., Naik S., Bhatt N., 2004, Nuclear Physics B Proc. Suppl., 132, 548
- Paul B., Raichur H., Naik S., Bhatt N., 2007, in Hayashida K., ed., The Extreme Universe in the Suzaku Era
- Paul, B., 2009, in Astrophysics with All-Sky X-Ray Observations, Proceedings of the RIKEN Symposium, p.362
- Porquet D., Grosso N., Goldwurm A., Sakano M., Belanger G., Ferrando P., Hasinger G., Aschenbach B., Prehel P., Tanaka Y., et al., 2007, ATel, 1058, 1
- Rappaport S., Verbunt F., Joss P., 1983, ApJ, 275, 713
- Ratti E. M., Bassa C. G., Torres M. A. P., Kuiper L., Miller-Jones J. C. A., Jonker P. G., 2010, MNRAS, 408, 1866
- Ruderman M., Shaham J., Tavani M., Eichler D., 1989, ApJ, 343, 292
- Singh N. S., Naik S., Paul B., Agrawal P. C., Rao A. R., Singh K. Y., 2002, A & A, 392, 161
- Tauris T. M., van den Heuvel E. P. J., 2006, in Compact Stellar X-ray Sources, ed. W. H. G. Lewin & M. van der Klis (Cambridge University Press), 623
- Wachter S., Smale A. P., Bailyn C., 2000, ApJ, 534, 367
- White N. E., Swank J. H., 1982, ApJ, 253, L61
- Wolff M. T., Hertz P., Wood K. S., Ray P. S., Bandyopadhyay R. M., 2002, ApJ, 575, 384
- Wolff M. T., Ray P. S., Wood K. S., Hertz P. L., 2009, ApJS, 183, 156